Redox Properties of Phosphazene Polymers with Pendant Ferrocene Groups

A. L. Crumbliss,*,† D. Cooke,† J. Castillo,‡ and P. Wisian-Neilson*,‡

Departments of Chemistry, Duke University, Durham, North Carolina 27708, and Southern Methodist University, Dallas, Texas 75275-0314

Received July 23, 1993®

The electrochemistry of a series of phosphazene polymers $\{[Ph(Me)=N]_x[Ph\{R'RC(OH)CH_2\}P=N]_y\}_n$ where R' is $(\eta^5\text{-}C_5H_4)Fe(\eta^5\text{-}C_5H_5)$ with varying degrees of ferrocene substitution (**3**, $x = 0.94$, $y = 0.06$, R = H; **4**, $x = 0.80$, $y = 0.20$, R = H; **5**, $x = 0.64$, $y = 0.36$, R = CH_3; **6**, $x = 0.56$, $y = 0.44$, R = H) has been investigated in CH_2Cl_2 and as films evaporatively deposited on the electrode surface. The $E_{1/2}$ of the ferrocene units (463 ± 12 mV *vs* Ag/AgCl) for the polymer dissolved in CH_2Cl_2 is essentially independent of the degree of substitution and background electrolyte. Diffusion coefficients (D_o) for **3–6** were determined using a combination of rotating-disk voltammetry and chronocoulometry. A trend of increasing D_o with increasing degree of ferrocene substitution suggests a dual mode of transport, where both physical diffusion and electron hopping are occurring. Polymer films were deposited by evaporation on Pt and glassy C electrodes, and $E_{1/2}$ values were measured at 470 ± 10 mV (Ag/AgCl) when the films were immersed in 0.1 M TBAP, (TBA)PF_6, TEAP, or (TEA)Br in acetonitrile or in TBAP or (TBA)PF_6 in CH_2Cl_2. Film-casting parameters were found to influence polymer swelling and charge-transport numbers ($D_o^{1/2}C$), which vary with the degree of ferrocene substitution from 1×10^{-7} to 5×10^{-9} mol/(cm^2 s$^{1/2}$).

Introduction

The electrochemistry of a variety of redox-active polymers has been investigated, and many of these materials have potential applications as electrode coatings and electrode mediators.[1-7] These studies include a number of inorganic (non-carbon backbone) polymers, such as the ferrocenyl-substituted polyphosphazenes **1** and **2**.[8]

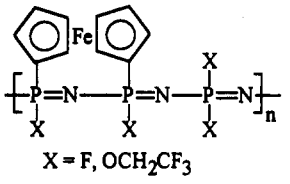

1

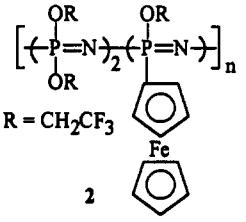

2

The use of redox-active polymers in solution and as film electrode coatings requires an understanding of the mechanism of charge transport. Modes of charge transport and diffusion through polymers in solution and those coated on an electrode have been extensively studied.[9-22] It is generally agreed that diffusion can occur *via* two possible mechanisms, physical diffusion and electron hopping. In solution, physical diffusion usually predominates, particularly for small molecules. For large polymers, the size of the molecule may diminish the contribution due to physical diffusion. Multiple redox sites incorporated in the polymer may enhance the contribution to diffusion due to electron hopping.

Previous investigators have reported the electrochemistry of ferrocene-substituted phosphazene cyclic trimers[23] and polymer films.[8] Charge-transport characteristics of the polymer films vary between structures **1** and **2** in such a way as to suggest the possible influence of ferrocene substituent mobility. In structure **1** the ferrocene substituent is fixed on the polymer chain, while in **2** it is more free to rotate as a side chain. In addition, the Langmuir voids in these polymer films may be sufficiently small to hinder the diffusion of the counterions from solution into the film to maintain electroneutrality.

Recently, a synthetic route was developed to prepare phosphazene polymers with a variable number of ferrocene substituents attached to the polymer backbone by flexible carbon spacer groups (eq 1).[24] We report here the electrochemical investigation of four such polymers in which 6–44% of the backbone units are substituted with ferrocenyl moieties, *i.e.*, polymers **3–6**. The fact that the ferrocene units are not a part of the polymer backbone and the spacing between the ferrocene units can be varied makes this an excellent series of polymers with which to probe the mechanism for electron transport within the polymer.

† Duke University.
‡ Southern Methodist University.
• Abstract published in *Advance ACS Abstracts,* November 15, 1993.

(1) *Inorganic and Organometallic Polymers*; Zeldin, M., Wynne, K., Allcock, H. R., Eds.; ACS Symposium Series 360; American Chemical Society: Washington, DC, 1988.
(2) Mark, J. E.; Allcock, H. R.; West, R. *Inorganic Polymers*; Prentice Hall: Englewood Cliffs, NJ, 1992.
(3) Sheats, J. E.; Carraher, C. E.; Pittman, C. U. *Metal Containing Polymer Systems*; Plenum: New York, 1985.
(4) Heinze, J. *Synth. Met.* **1991**, *41–43*, 2805.
(5) Doblhofer, K.; Zhong, C. *Synth. Met.* **1991**, *41–43*, 2865.
(6) Andrieux, C. P.; Saveant, J. M. *Tech. Chem. (N.Y.)* **1992**, *22*, 159.
(7) Wrighton, M. S. *Science* **1986**, *231*, 32.
(8) Saraceno, R. A.; Riding, G. H.; Allcock, H. R.; Ewing, A. G. *J. Am. Chem. Soc.* **1988**, *110*, 7254.
(9) Murray, R. W. In *Electroanalytical Chemistry*; Bard, A. J., Ed.; Marcel Dekker: New York, 1984; Vol. 13, p 191.
(10) Surridge, N. A.; Jernigan, J. C.; Dalton, E. F.; Buck, R. P.; Watanabe, M.; Zhang, H.; Pinkerton, M.; Wooster, T. T.; Longmure, M. L.; Facci, J. S.; Murray, R. W. *Faraday Discuss. Chem. Soc.* **1989**, *88*, 1.
(11) Faulkner, L. R. *Electrochim. Acta* **1989**, *34*, 1.
(12) Fritsch-Faules, I.; Faulkner, R. L. *J. Electroanal. Chem. Interfacial Electrochem.* **1989**, *263*, 237.
(13) Oh, S. M.; Faulkner, L. R. *J. Electroanal. Chem. Interfacial Electrochem.* **1989**, *269*, 77.
(14) Pinkerton, M. J.; Le Mest, Y.; Zhang, H.; Watanabe, M.; Murray, R. W. *J. Am. Chem. Soc.* **1990**, *112*, 3730.
(15) Dalton, E. F.; Surridge, N. A.; Jernigan, J. C.; Wilbourn, K. O.; Facci, J. S.; Murray, R. W. *Chem. Phys.* **1990**, *141*, 143.
(16) Bowden, E. F.; Dautortas, M. F.; Evans, J. F. *J. Electroanal. Chem. Interfacial Electrochem.* **1987**, *219*, 49.
(17) Doblhofer, K.; Durr, W.; Jauch, M. *Electrochim. Acta* **1982**, *27*, 677.
(18) Dahms, H. *J. Phys. Chem.* **1968**, *72*, 362.
(19) Ruff, I. *Electrochim. Acta* **1970**, *15*, 1059.
(20) Ruff, I.; Friedrich, V. J. *J. Phys. Chem.* **1971**, *75*, 3297.
(21) Ruff, I.; Friedrich, V. J.; Demeter, H.; Csillag, K. *J. Phys. Chem.* **1971**, *75*, 3303.
(22) Murray, R. W. *Annu. Rev. Mater. Sci.* **1984**, *14*, 145.
(23) Saraceno, R. A.; Riding, G. H.; Allcock, H. R.; Ewing, A. G. *J. Am. Chem. Soc.* **1988**, *110*, 980.
(24) Wisian-Neilson, P.; Ford, R. R. *Organometallics* **1987**, *6*, 2258.

0020-1669/93/1332-6088$04.00/0

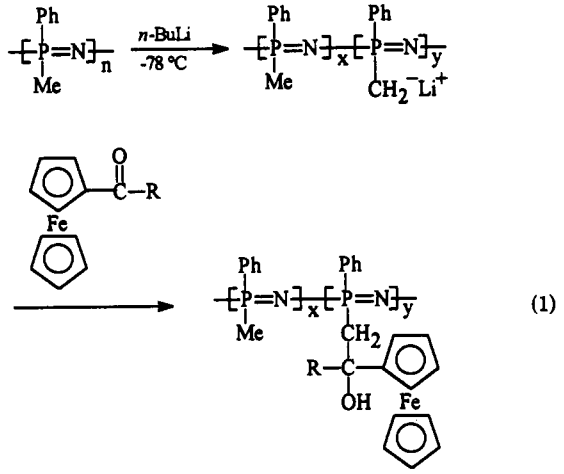

(1)

3, $x = 0.94$, $y = 0.06$, R = H
4, $x = 0.80$, $y = 0.20$, R = H
5, $x = 0.64$, $y = 0.36$, R = CH_3
6, $x = 0.56$, $y = 0.44$, R = H

Experimental Section

Materials. Tetraethylammonium perchlorate, TEAP (Southwestern Analytical Chemical), tetrabutylammonium perchlorate, TBAP (Kodak), tetraethylammonium bromide, (TEA)Br (Aldrich), tetrabutylammonium hexafluorophosphate, $(TBA)PF_6$ (Aldrich), acetonitrile (Kodak), and dichloromethane (Kodak) were all used as received.

Polymer Synthesis. Details of the synthesis of ferrocenyl-substituted polymers were reported earlier,[25] but here stoichiometries were varied to alter the degree of ferrocene substitution. Typically, the amount of *n*-BuLi used was somewhat higher than the actual degree of substitution in the final polymer. For example, polymers **3** and **4** were prepared by treating 2.2 g (16 mmol) of $[Me(Ph)PN]_n$ with 1.6 mL (4 mmol) and 2.6 mL (6.5 mmol) of 2.5 M *n*-BuLi in hexane, respectively. The polymer anions formed in this fashion were then treated with equimolar quantities of either ferrocenecarboxaldehyde or acetylferrocene and the reactions were quenched with *ca.* 2 mL of saturated NH_4Cl. Purification involved precipitation from THF into water and then from THF into hexane and finally by at least 10 h of Soxhlet extraction with ethanol. The polymers were dried for a minimum of 18 h under vacuum at 50 °C. The ^1H and ^{31}P NMR and IR spectra for each polymer were similar, with varying intensities of signals corresponding to different degrees of substitution. Representative spectroscopic data: IR 3350 (s, br, OH), 1150 (m, C—O), 1180 cm^{-1} (s, vbr, P=N); ^1H NMR δ 0.9–2.3 (PCH_2, PCH_3, and for **5** CCH_3), 3.8–4.0 ($C_5H_4C_5H_5$), 4.5 (*H*COH; **3**, **4**, and **6** only), 6.0–6.5 (OH), 7.0–7.8 (C_6H_4); ^{31}P NMR δ 2.3, 5.6, with the latter increasing in intensity from **3** to **6**.

Elemental Analyses and Molecular Weight Data. Polymer **3**: Anal. Calcd for $x = 0.94$, $y = 0.06$; C, 61.35; H, 5.78; N, 9.34. Found: C, 60.31; H, 6.05; N, 8.96. T_g = 40 °C. M_w = 83 000, M_n = 51 000. Polymer **4**: Anal. Calcd for $x = 0.80$, $y = 0.20$; C, 61.41; H, 5.60; N, 7.78. Found: C, 59.94; H, 5.53; N, 7.21. T_g = 70 °C. M_w = 253 000, M_n = 83 000. Polymer **5**: Anal. Calcd for $x = 0.64$, $y = 0.36$; C, 62.02; H, 5.66; N, 6.39. Found: C, 61.85; H, 5.94; N, 6.39. T_g = 87 °C. M_w = 264 000, M_n = 154 000. Polymer **6**: Anal. Calcd for $x = 0.56$, $y = 0.44$; C, 61.48; H, 5.40; N, 6.06. Found: C, 61.39; H, 5.63; N, 5.40. T_g = 89 °C. M_w = 147 000, M_n = 81 000. Polymers **3**, **4**, and **6** were prepared from $[Me(Ph)PN]_n$ with M_w = 78 000, M_n = 48 000, and **5** was made from a sample with M_w = 159 000, M_n = 98 000.

Methods. Polymer Characterization. Elemental analyses were performed using a Carlo Erba Strumentazione 1106 CHN elemental analyzer. Gel permeation chromatography measurements were performed using a Waters Associate GPC instrument with Maxima solftware for data handling using μ styragel columns (500, 10^3, 10^4, 10^5 Å). The SEC operating conditions consisted of a mobile phase of THF containing 0.1% $(n\text{-}Bu)_4N^+Br^-$, a flow rate of 1.5 mL/min, a temperature of 30 °C, and a sample size of 50 μL of 0.1% solution. Calibration was accomplished with a series of narrow molecular weight polystyrene standards. The ^1H and ^{31}P NMR spectra were recorded using an IBM WP-200SY FT NMR spectrometer in $CDCl_3$. Positive ^1H NMR resonances are downfield from the external reference Me_4Si, and positive ^{31}P NMR resonances are downfield from the external reference phosphoric acid. IR spectra were recorded as thin films or as $CDCl_3$ solutions using a Perkin-Elmer 283 spectrometer. Differential scanning calorimetry (DSC) measurements were made under nitrogen using a Du Pont 910 instrument with an aluminum reference and a temperature range of 0–150 °C. Each sample was heated and cooled at least two times. The glass transition temperatures reported are the inflection points for the final heating cycle.

Electrochemical Apparatus. Cyclic voltammetry (CV), chronocoulometry (CC), and chronoamperometry (CA) were performed using a BAS CV-27 potentiostat. Rotating-disk voltammetry (RDV) was performed using a Pine AFMSRX modulated-speed rotator and a BAS CV-27 potentiostat. The electrochemical cell was a conventional three-electrode arrangement with a Pt wire as an auxiliary electrode, a silver/silver chloride reference electrode, and either a glassy carbon or a platinum disk working electrode. The glassy carbon (r = 0.8 mm for CV and CA), pyrolytic graphite (r = 0.25 cm for CC and RDV), and platinum disk (r = 0.7 mm for CV and CA) electrodes gave similar results, although the lifetime of the polymer film was longer on the glassy carbon electrode. The working electrodes for CV and CA were polished with alumina on a polishing wheel. The working electrode for CC and RDV was cleaned by soaking the electrode in 0.1 M HNO_3 for 10 min. All CV scans were done in a solution of background electrolyte dissolved in acetonitrile (polymer film) or dichloromethane (solution studies). For solution studies, the electrode was removed from solution and polished before each CV scan was recorded, and before each CC measurement was made, to minimize adsorption. CC plots of charge as a function of the square root of time passed through the origin within experimental error, which is consistent with a lack of polymer adsorption to the electrode surface. The $E_{1/2}$ values were calculated from the anodic and cathodic peak potentials; $E_{1/2} = (E_{pa} - E_{pc})/2$.

Preparation of Polymer Film Coated Electrodes. Polymer film deposition methods were optimized with respect to longevity of the film on the electrode surface. The polymers were dissolved in a solution of dichloromethane containing 0.1 M TBAP in similar milligram proportions so as to roughly reflect the current changes due to the changes in ferrocene substitution. Six drops of this solution were placed on a freshly polished glassy carbon electrode and allowed to evaporate to dryness. All subsequent scans were done in acetonitrile containing 0.1 M TEAP. The lifetime of the polymer film on the glassy carbon electrode was 4 h, compared with 1–2 h for the platinum electrode. Several experiments were done in which both the background electrolyte that was evaporatively deposited onto the electrode and the background electrolyte present in the contact solution were changed. The electrolytes used other than TEAP were tetraethylammonium bromide ((TEA)Br), tetrabutylammonium perchlorate (TBAP), and tetrabutylammonium hexafluorophosphate ($(TBA)PF_6$). Literature reports suggest that changing the counterions will influence charge transport through the film[26] and voltammogram asymmetry.[27] The optimum system was determined to be that of the polymer evaporated with TBAP and scanned in 0.1 M TEAP in acetonitrile. Relatively poor quality films resulted from evaporative deposition from solutions that did not contain background electrolyte.

Diffusion Coefficient and Charge-Transport-Number Calculations. A combination of RDV and CC experiments were performed in order to eliminate uncertainties in the calculation of diffusion coefficients for the polymer in solution. The uncertainty arises due to the range in the molecular weights for each polymer sample (and therefore the polymer concentration (C)) and the uncertainty in the number of electrons transferred (n) per polymer molecule. The Levich equation for RDV[28] (eq 2) shows the relationship between the rotation speed and the limiting

$$i_l = 0.620nFAD_o^{2/3}\omega^{1/2}\nu_{rdv}^{-1/6}C \qquad (2)$$

i_l = limiting current
n = number of electrons transferred
A = area of the working electrode
F = Faraday's constant
D_o = diffusion coefficient
ω = rotation speed
ν_{rdv} = kinematic viscosity
C = concentration

current. This linear relationship applies when the kinetics are rapid and

(25) Wisian-Neilson, P.; Ford, R. R. *Macromolecules* **1989**, *22*, 72.

when the correct electrode rotation speed window is used (*e.g.*, there is no turbulence or vortex formation). The Anson or integrated Cottrell equation for chronocoulometry[28] (eq 3) describes a linear relationship

$$Q_d = (2nFAD_o^{1/2}Ct^{1/2})/(\pi^{1/2}) \quad (3)$$

Q_d = charge of the diffusing species
n = number of electrons transferred
F = Faraday's constant
A = area of the working electrode
D_o = diffusion coefficient
C = concentration of redox species
t = time

between the charge at the electrode and time. A plot of eq 3 is linear for a diffusion-controlled process. When eqs 2 and 3 are solved for $nFAC$, they can be set equal to each other. The resulting equation can then be solved for the diffusion coefficient without considering the concentration (C) or the number of electrons transferred (n) as variables.[29] The net equation, used to calculate the diffusion coefficients in this study from RDV and CC data is

$$D_o^{1/6} = [2(\text{slope})_{rdv}]/[0.620\pi^{1/2}\nu_{rdv}^{-1/6}(\text{slope})_{cc}] \quad (4)$$

where $(\text{slope})_{rdv}$ represents the slope of the i_l *vs* $\omega^{1/2}$ plot obtained from RDV and $(\text{slope})_{cc}$ represents the slope of the Q_d *vs* $t^{1/2}$ plot obtained from CC.

Charge-transport numbers, $D_o^{1/2}C$, for the polymer films deposited on the electrode surface were calculated from the slopes of peak current *vs* the square root of the scan rate plots for cyclic voltammetry over the range 75–200 mV/s, using the Randles–Sevcik equation (eq 5)[28] and

$$i_p = (2.69 \times 10^5)n^{3/2}AD_o^{1/2}C\nu_{cv}^{1/2} \quad (5)$$

i_p = peak current
n = number of electrons transferred
A = area of the electrode
D_o = diffusion coefficient
C = concentration of redox species
ν_{cv} = scan rate

assuming $n = 1$. Surface coverage, Γ, was calculated on the basis of the slope of the peak current *vs* scan rate plot over the range 5–50 mV/s assuming $n = 1$ in eq 6.[28]

$$i_p = (n^2F^2\nu_{cv}A\Gamma)/(4RT) \quad (6)$$

i_p = peak current
n = number of electrons transferred
F = Faraday's constant
A = area of the electrode
Γ = surface coverage of redox species
R = gas constant
T = temperature
ν_{cv} = scan rate

Error assignments for $D_o^{1/2}C$ and Γ are based on uncertainties in the slope (standard deviation) of a linear regression. Error assignments for D_o and $E_{1/2}$ are the standard deviation of an average of three to six independent determinations.

(26) Nowak, R. J.; Schultz, F. A.; Umana, M.; Lam, R.; Murray, R. W. *Anal. Chem.* **1980**, *52*, 315.
(27) Peerce, P. J.; Bard, A. J. *J. Electroanal. Chem. Interfacial Electrochem.* **1980**, *114*, 89.
(28) Bard, A. J.; Faulkner, L. R. *Electrochemical Methods: Fundamentals and Applications*; Wiley: New York, 1982.
(29) Tieman, R. S.; Coury, L. A., Jr.; Kirchoff, J. R.; Heinemann, W. R. *J. Electroanal. Chem. Interfacial Electrochem.* **1990**, *281*, 133.

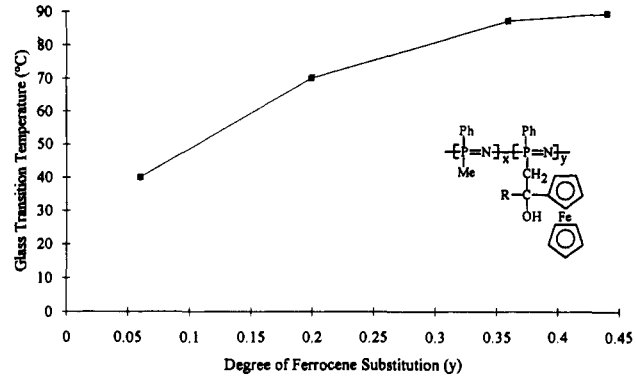

Figure 1. Plot of glass transition temperature as a function of degree of ferrocene substitution.

Results

Polymer Synthesis and Characterization. The ferrocene-substituted polymers (eq 1) were characterized by NMR and IR spectroscopy and by elemental analysis. The degree of ferrocene substitution was calculated by integration of the ^{1}H NMR spectra and was verified by elemental analysis. The polymers were carefully purified to remove NH_4Cl and unreacted ferrocenecarboxaldehyde or acetylferrocene. Molecular weights were estimated by gel permeation chromatography (GPC). As expected for incorporation of the ferrocene moieties, these values are slightly higher than those of the parent polymers from which they were prepared.[30] Figure 1 is a plot of the glass transition temperature (T_g) as a function of the degree of ferrocene substitution (*i.e.*, as the ratio y:x is increased). Glass transition temperatures reflect the torsional mobility of the polymer backbone, and Figure 1 illustrates that the torsional mobility of the ferrocene-substituted phosphazene polymers decreases with increasing ferrocene substitution. This is likely due to both the steric bulk of the ferrocene group and hydrogen bonding of the hydroxy groups.

Solution Studies. Phosphazene polymers **3–6** were readily oxidized and re-reduced at a platinum or glassy carbon electrode surface when dissolved in CH_2Cl_2 in the presence of background electrolyte. Cyclic voltammetry (CV), rotating disk voltammetry (RDV), and chronocoulometry (CC) were used to characterize the four different ferrocene-substituted phosphazene polymers in CH_2Cl_2 solution. Chemically reversible cyclic voltammograms were obtained, and representative examples are illustrated in Figure 2. The $E_{1/2}$ values, obtained from cyclic voltammetry, are listed in Table I. In each case, plots of peak current as a function of the square root of the scan rate were linear over the scan rate range from 5 to 200 mV/s, indicating that charge transfer is similar to a linear diffusion process as described by the Randle–Sevcik equation.[28]

Diffusion coefficients for each polymer sample were obtained using rotating-disk voltammetry to generate plots of limiting current (i_l) as a function of the square root of the electrode rotation speed ($\omega^{1/2}$) and chronocoulometry to generate plots of charge as a function of the square root of the time. Representative data are shown in Figures 3 and 4. As described in the Experimental Section, this procedure eliminates the necessity for using molar concentration and the number of electrons transferred per molecule in calculating experimental diffusion coefficients, thus eliminating a major source of uncertainty.[29] Table I lists the diffusion coefficients for each polymer sample in CH_2Cl_2. Also included in Table I are $E_{1/2}$ and D_o values for the monomer redox unit, ferrocenemethanol, obtained under our conditions for comparison purposes.

(30) Absolute molecular weights for the parent polymer, $[Me(Ph)PN]_n$, have been determined: Neilson, R. H.; Hani, R.; Wisian-Neilson, P.; Meister, J. J.; Roy, A. K.; Hagnauer, G. L. *Macromolecules* **1987**, *20*, 910.

Table I. Electrochemistry of Ferrocene-Substituted Phosphazene Polymers in Solution

polymer	$E_{1/2}$, mV[a]	ΔE_{pp}, mV[b]	D_o, cm^2/s[c]
3	447(5)	121(3)	1.5×10^{-13}
4	477(15)	70(5)	2.5×10^{-10}
5	464(3)	62(3)	7.5×10^{-10}
6	464(8)	55(9)	1.4×10^{-8}
ferrocenemethanol[d]	435(5)	72(6)	2.3×10^{-5}

[a] 1.0–1.5 mg of polymer/mL of CH_2Cl_2/0.1 M TEAP. Data obtained from cyclic voltammetry using a Pt disk electrode. The $E_{1/2}$ values are relative to Ag/AgCl reference and are an average of three or four independent determinations at 20 mV/s. Numbers in parentheses represent standard deviations. [b] 1.0–1.5 mg of polymer/mL of CH_2Cl_2/0.1 M TEAP. Peak separation data obtained from cyclic voltammetry using a platinum disk electrode and a scan rate of 20 mV/s. Values are an average of three or four independent determinations with standard deviations in parentheses. [c] Calculated from eq 4 using data obtained in 0.1 M TEAP/CH_2Cl_2 as described in the Experimental Section. Total bulk concentrations of ferrocene substituents were 3.1×10^{-4}, 8.5×10^{-4}, 1.0×10^{-3}, and 1.4×10^{-3} M for polymers 3–6, respectively. [d] Monomer.

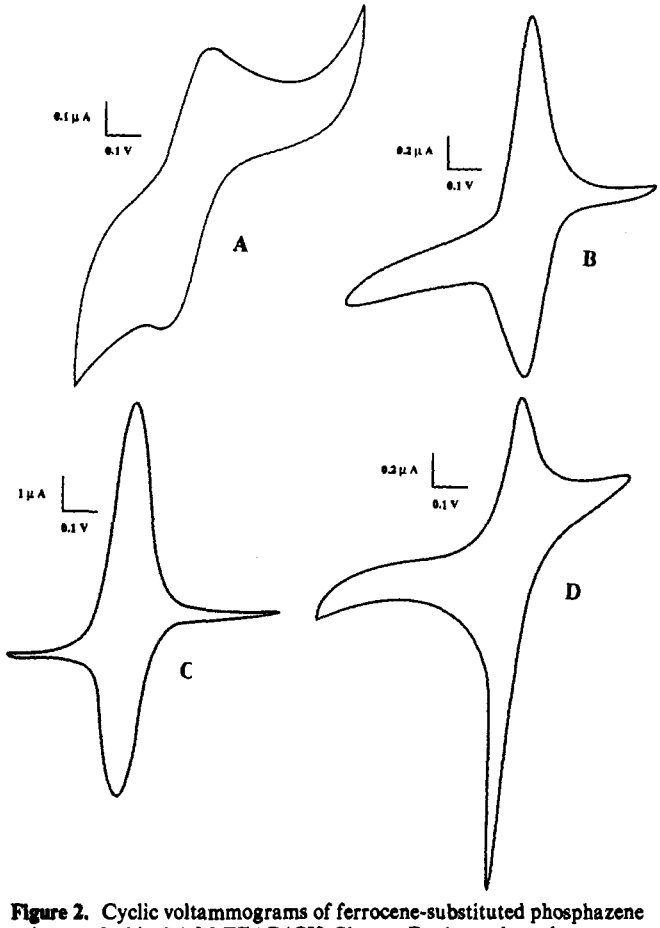

Figure 2. Cyclic voltammograms of ferrocene-substituted phosphazene polymers 3–6 in 0.1 M TEAP/CH_2Cl_2 at a Pt electrode and scan rate of 20 mV/s: (A) 1.5 mg of 3/mL; (B) 1.3 mg of 4/mL; (C) 1.5 mg of 5/mL; (D) 1.1 mg of 6/mL.

Film Studies. Ferrocene-substituted phosphazene polymer films were deposited on glassy carbon electrodes as described in the Experimental Section. These polymer films can be electrochemically oxidized and re-reduced when in contact with a variety of electrolyte/solvent systems. The polymer films were characterized by cyclic voltammetry in acetonitrile containing 0.1 M TEAP. All four polymer films exhibited a "break-in" period over the first one to four potential scans. The cyclic voltammograms initially produced were asymmetric with a cathodic to anodic peak ratio less than 1. This ratio approached unity with repetitive scans. In addition to this initial asymmetry, the anodic peak was very sharp. This sharpness diminished with increasing scans, indicating a change in the polymer morphology. The break-in period is attributed to a swelling of the polymer to its equilibrium state. After the break-in period the films were stable for over 4 h of repeated potential scans in CH_3CN, as evidenced by invariant voltammograms. Representative cyclic voltammograms are shown in Figure 5. The $E_{1/2}$ values obtained from cyclic voltammetry of the polymer films are listed in Table II. The small peak to peak separations, from a low of 1 mV at a scan rate of 20 mV/s to a high of 330 mV at 200 mV/s, indicate electrode surface bound redox behavior. This is compared to the cases of other ferrocene-substituted phosphazene films where a peak to peak separation range was observed from 100 mV to 1.24 V.[8]

A similar break-in period has been observed for several polymerized vinylferrocene films.[31] Murray and Daum attributed this to the movement of the charge-compensating anions.[32] They

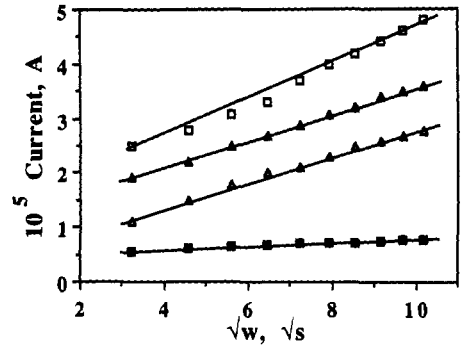

Figure 3. Plots of anodic limiting current (i_l) as a function of electrode rotation speed ($\omega^{1/2}$) for ferrocene-substituted phosphazene polymers 3 (■), 4 (△), 5 (▲), 6 (□).

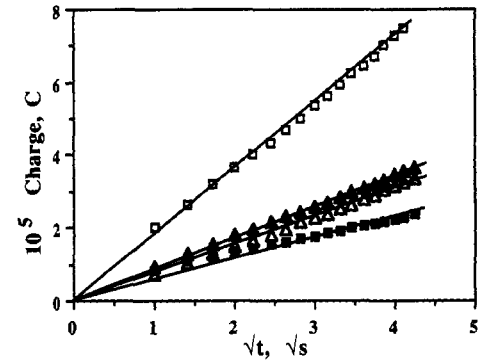

Figure 4. Plots of charge as a function of the square root of time for ferrocene-substituted phosphazene polymers 3 (■), 4 (△), 5 (▲), and 6 (□).

Table II. Electrochemistry of Ferrocene-Substituted Phosphazene Polymer Films[a]

polymer	$E_{1/2}$, mV[b]	ΔE_{pp}, mV[c]	$D_o^{1/2}C$, mol/(cm^2 s$^{1/2}$)[d] cathodic	$D_o^{1/2}C$, mol/(cm^2 s$^{1/2}$)[d] anodic	Γ, mol/cm^2 [e]
3	461(1)	3(1)	$5.7(0.8) \times 10^{-9}$	$1.2(0.2) \times 10^{-8}$	$1.1(0.4) \times 10^{-9}$
4	478(3)	1(1)	$1.2(0.4) \times 10^{-7}$	$9.0(0.5) \times 10^{-8}$	$8.9(0.4) \times 10^{-9}$
5	461(5)	1(1)	$6.1(0.6) \times 10^{-7}$	$8.4(0.7) \times 10^{-7}$	$2.1(0.4) \times 10^{-9}$
6	478(2)	18(7)	$1.7(0.2) \times 10^{-8}$	$1.2(0.6) \times 10^{-8}$	$1.0(0.8) \times 10^{-9}$

[a] Film deposited by evaporation on a glassy carbon electrode. [b] Data obtained from cyclic voltammetry in 0.1 M TEAP/CH_3CN at 20 mV/s scan rate. The $E_{1/2}$ values are relative to Ag/AgCl reference and are an average of three to five independent determinations. The numbers in parentheses represent standard deviations. [c] Peak separation data obtained from cyclic voltammetry at a scan rate of 20 mV/s. Values are an average of three to six independent determinations, and standard deviations are listed in parentheses. [d] Charge-transport numbers in 0.1 M TEAP/CH_3CN calculated from data obtained over a scan range of 75–200 mV/s using eq 5 as described in the Experimental Section. Error limits are defined by linear regression analysis. [e] Film surface coverage expressing surface concentration of redox sites calculated from data obtained over a scan rate range of 5–50 mV/s using eq 6 is described in the Experimental Section. Error limits are defined by linear regression analysis.

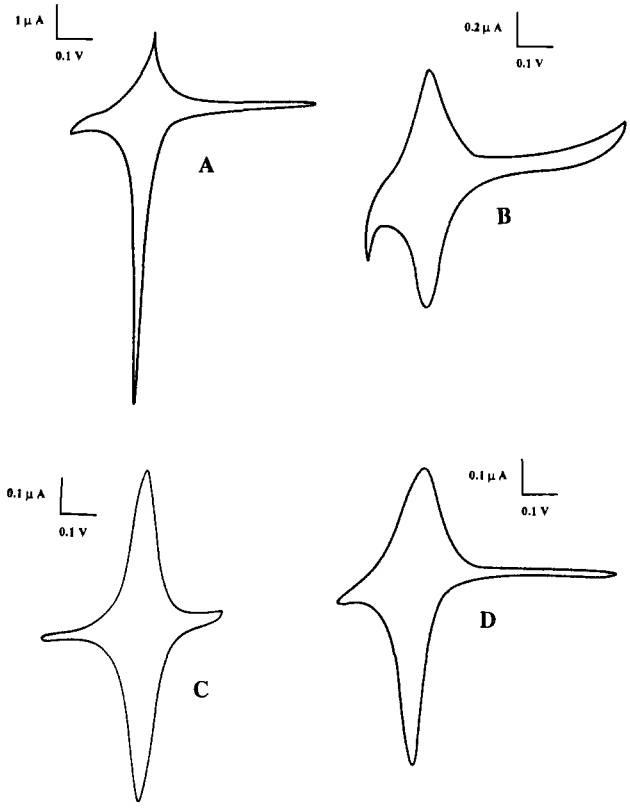

Figure 5. Cyclic voltammograms of ferrocene-substituted phosphazene polymer films on glassy carbon electrodes in 0.1 M TEAP/CH_3CN recorded after a break-in period of four or five scans at a scan rate of 20 mV/s: (A) **3**, $\Gamma = 3.3 \times 10^{-9}$ mol/cm^2, $D_o^{1/2}C_{cathodic} = 3.4 \times 10^{-9}$ mol/(cm^2 s$^{1/2}$), $D_o^{1/2}C_{anodic} = 6.2 \times 10^{-9}$ mol/(cm^2 s$^{1/2}$); (B) **4**, $\Gamma = 1.8 \times 10^{-9}$ mol/cm^2, $D_o^{1/2}C_{cathodic} = 7.4 \times 10^{-8}$ mol/(cm^2 s$^{1/2}$), $D_o^{1/2}C_{anodic} = 7.8 \times 10^{-8}$ mol/(cm^2 s$^{1/2}$); (C) **5**, $\Gamma = 6.3 \times 10^{-9}$ mol/cm^2, $D_o^{1/2}C_{cathodic} = 2.2 \times 10^{-7}$ mol/(cm^2 s$^{1/2}$), $D_o^{1/2}C_{anodic} = 5.7 \times 10^{-7}$ mol/(cm^2 s$^{1/2}$); (D) **6**, $\Gamma = 5.2 \times 10^{-9}$ mol/cm^2, $D_o^{1/2}C_{cathodic} = 8.9 \times 10^{-9}$ mol/(cm^2 s$^{1/2}$), $D_o^{1/2}C_{anodic} = 7.9 \times 10^{-9}$ mol/(cm^2 s$^{1/2}$).

also noted that it is dependent on the solvent. In fact, we observe anodic peak sharpness only in acetonitrile and not in CH_2Cl_2. This can be explained by the solvent's ability to swell the polymer.

Surface coverage and charge-transport numbers for each polymer film are also listed in Table II. Due to the uncertainty of C, it is difficult to make comparisons regarding the $D_o^{1/2}C$ and surface coverage, Γ. However, there was no significant difference between the $D_o^{1/2}C$ values calculated from anodic and cathodic data.

Figure 6 is a representative plot of the influence of scan rate on the peak current for the polymer film on a glassy carbon electrode surface. At low scan rates, 1 mV/s to a high of 50 mV/s in some cases, the peak current varies linearly with scan rate, consistent with electrode surface bound redox behavior. At higher scan rates (50–200 mV/s), the peak current varies linearly with the square root of the scan rate, consistent with a diffusion-controlled process. That is, the charge transport through the film is influenced by background electrolyte diffusion into and out of the film. Consequently, charge-transport efficiency will likely be influenced by film thickness and morphology, as well as the identity of the diffusing ions (background electrolyte).[33] The following example serves to illustrate the influence of film thickness. Two drops of a CH_2Cl_2 solution containing 84 mg of **5** and 0.1 M TEAP gave a redox species surface coverage of 3.0(0.3) $\times 10^{-8}$ mol/cm^2, and four drops of the same solution

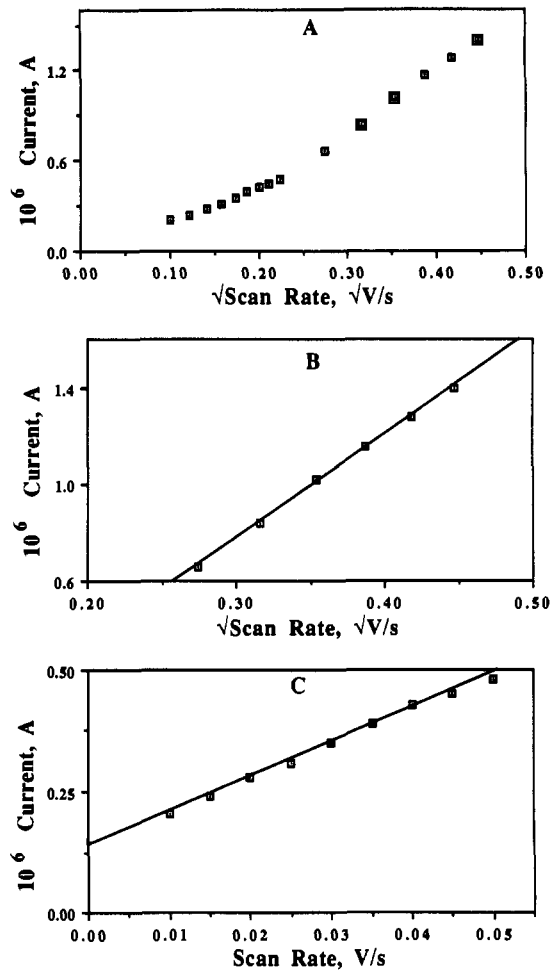

Figure 6. Plots of cathodic and anodic peak currents for ferrocene-substituted phosphazene polymer film **5** on the surface of a glassy carbon electrode in contact with 0.1 M TEAP/CH_3CN: (A) peak current *vs* square root of the scan rate over the scan rate range 5–200 mV/s; (B) peak current *vs* square root of the scan rate over the scan rate range 75–200 mV/s; (C) peak current *vs* scan rate over the scan rate range 5–50 mV/s.

yielded a surface coverage of 4.6(0.4) $\times 10^{-8}$ mol/cm^2. The efficiency of charge transport through the film was found to decrease with this modest increase in surface coverage, as seen by the decrease in charge-transport rate ($D_o^{1/2}C$) from 2.3(0.2) $\times 10^{-7}$ to 9.5(0.7) $\times 10^{-9}$ mol/(cm^2 s$^{1/2}$).

Discussion

Redox Potentials. Well-behaved cyclic voltammograms were obtained for all polymers investigated, both in solution and as solid films. This illustrates a facile oxidation and re-reduction of the pendant ferrocene groups. Substituents on the cyclopentadienyl ring are known to influence the redox potential of ferrocene in a regular manner, with electron-withdrawing groups shifting the potential positive and electron-donating groups shifting the potential negative, relative to unsubstituted ferrocene.[34-36] Reversible $E_{1/2}$ values were not reported for the ferrocene-substituted phosphazene polymers **1** and **2**.[8] However, the electronic influence of the phosphazene polymer on the redox properties of the ferrocene was estimated by these authors by considering a series of ferrocene-substituted cyclic phosphazenes.[23]

(31) Yang, E. S.; Chan, M.; Wahl, A. C. *J. Phys. Chem.* **1980**, *84*, 3094.
(32) Daum, P.; Murray, R. W. *J. Electroanal. Chem. Interfacial Electrochem.* **1979**, *103*, 289.
(33) Daum, P.; Lenhard, J. R.; Rolison, D.; Murray, R. W. *J. Am. Chem. Soc.* **1980**, *102*, 4649.
(34) Little, W. F.; Reilly, C. N.; Johnson, J. D.; Lynn, K. N.; Sanders, A. P. *J. Am. Chem. Soc.* **1964**, *86*, 1376.
(35) Little, W. F.; Reilly, C. N.; Johnson, J. D.; Sanders, A. P. *J. Am. Chem. Soc.* **1964**, *86*, 1382.
(36) Fultz, M. L.; Durst, R. A. *Anal. Chim. Acta* **1982**, *140*, 1 and references therein.

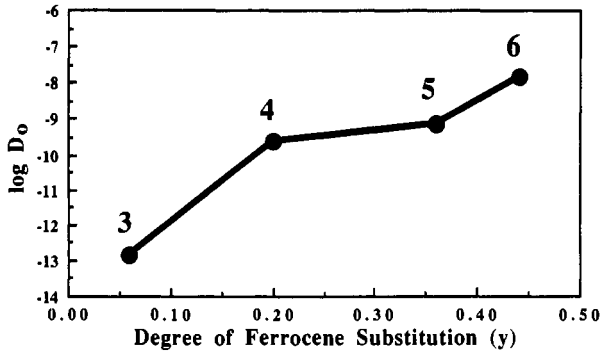

Figure 7. Plot of the log of the diffusion coefficient for each of the ferrocene-substituted polymers (**3–6**) in 0.1 M TEAP/CH_2Cl_2 solution as a function of the degree of substitution.

Phosphazene substitution results in anodic peak potentials that are shifted 280–780 mV positive of the unsubstituted ferrocene monomer.[23] This suggests an electron-withdrawing effect for the phosphazene polymer when bound directly to the cyclopentadienyl ring. The $E_{1/2}$ values for the ferrocene-substituted phosphazene polymers reported here, although shifted slightly positive, are comparable to that observed for ferrocenemethanol (Table I). This is consistent with a much diminished influence of the phosphazene backbone on the ferrocene redox couple in **3–6**, relative to the polymers **1** and **2**. The ferrocene moiety is removed from the phosphazene substituent by a two-carbon chain in the polymers reported here, which largely masks any electronic influence of the phosphazene backbone.

Charge Transport in Solution. It is widely accepted that the diffusion coefficient measured in solution is a combination of physical diffusion and diffusion *via* electron hopping, although the relative contributions of these two paths are often difficult to determine.[10,14,18–22] Physical diffusion for the phosphazene polymer can be assumed to be similar for all four polymer derivatives (**3–6**), due to the relative similarity in their molecular weights and structures. The diffusion of the bulky polymer chains should not be significantly affected by the number of ferrocene side chains. Certainly the observed 10^5 variation in solution diffusion coefficients (Table I) is too large to be accounted for by variations in polymer molecular weight, structure, or rigidity.

The value reported for the electron-self-exchange rate constant for ferrocene monomer in solution (10^7 M^{-1} s^{-1})[31,37] suggests that electron hopping may provide a significant contribution to the observed diffusion coefficients in Table I. The increase in D_o with increasing ferrocene substitution in polymers **3–6** (Figure 7) is consistent with a proximity effect between ferrocene units along the polymer chain. That is, electron hopping contributes more to the observed diffusion coefficient as the distance between pendant ferrocene groups decreases.

Equation 7[10,14,18–22] illustrates the parallel contributions of physical diffusion (D_{phys}) and electron hopping (D_e) to the experimentally observed diffusion coefficient (D_o), where δ is the

$$D_o = D_{phys} + D_e \tag{7}$$

$$D_e = \pi\delta^2 k_{app} C/4$$

$$k_{app}^{-1} = k_{ex}^{-1} + k_d^{-1}$$

distance between reaction pairs when electron exchange occurs, C is the concentration, k_{ex} is the self-exchange rate constant, and k_d is the diffusion-controlled electron-transfer rate constant. The trend illustrated in Figure 7 is certainly not a bulk concentration effect (as expressed in eq 7), since all of the experiments were done under conditions where the total bulk ferrocene concentrations varied by less than a factor of 5 (footnote *c*, Table I). The observed variation in D_o is a factor of 10^5. Assuming that D_{phys} may be approximated by the 10^{-13} cm^2 s^{-1} observed for D_o for **3** and substituting available parameters for ferrocene (δ = 7.08 × 10^{-8} cm;[21] k_{ex} = 10^7 M^{-1} s^{-1} [31,37]) into eq 7 result in a predicted electron-hopping term (D_e) which is too small. We conclude that eq 7 is not strictly applicable to our system and/or that k_{app} is enhanced by the close proximity of the ferrocene groups along the polymer chain, possibly by an increased frequency of collisions resulting in electron exchange.

Charge Transport through Films. Films of ferrocene-substituted phosphazene polymer undergo facile oxidation and reduction when coated on an electrode surface. Data in Table II illustrate that both anodic and cathodic charge-transport rates are of the same order of magnitude, suggesting little difference between the oxidation and reduction processes. Apparently any polymer swelling that occurs upon oxidation is reversible. This is also supported by the observed reversible electrochemistry. The similar charge-transport rates suggest that the oxidation/reduction processes proceed by the same mechanism in reverse.

The observed currents for the films are larger than can be accounted for by a monolayer of adsorbed polymer. Apparently a mechanism exists for transporting electrons through the phosphazene polymer film. This charge-transport process may be conceived as proceeding by a mechanism involving the following steps, any one of which may be rate determining.[33,38] Electrons may be transmitted through the film by hopping between adjacent ferrocene groups. This electron hopping results in an oxidation state change and requires the transport of charge-compensating counterions into and out of the film. This counterion flux may also be associated with solvent flow and polymer chain motion. Results related to each of these steps are discussed below.

Charge diffusion through the polymer film adsorbed on the electrode surface may be influenced by the degree of ferrocene substitution. A measure of the potential efficiency of the electron-hopping process is the self-exchange rate constant for ferrocene (10^7 M^{-1} s^{-1}).[31,37] Increasing the degree of ferrocene substitution in our phosphazene polymer can increase the efficiency of electron self-exchange by decreasing the distance between ferrocene groups (*i.e.*, increasing the concentration of redox centers). An increase in the number of polymer side groups may also increase the number of channels for electrolyte diffusion into and out of the film.

Data in Table II show that the charge-transport numbers ($D_o^{1/2}C$) for the films increase with increasing degree of ferrocene substitution in the sequence **3** < **4** < **5**. This may be a reflection of the increased efficiency of electron self-exchange between ferrocene units as the polymer chain distance between ferrocene units decreases. On the other hand, increased substitution of the large ferrocene units and increased possibilities of hydrogen bonding with larger numbers of OH groups can counteract the efficiency of electron transport by decreasing the ease of background electrolyte diffusion into and out of the film. This could explain the decreased charge-transport number for **6**. Data in Table II show that as the $D_o^{1/2}C$ values decrease on going from **5** to **6**, the peak to peak separations in the cyclic voltammograms significantly increase. This suggests that, for **6**, polymer morphology and background electrolyte diffusion into and out of the film may be more important contributions to charge transport, relative to electron exchange between ferrocene side chains. Polymer film morphology is undoubtedly influenced by increasing the number of side chains. Polymer backbone rigidity is also a factor which varies with ferrocene substitution, as illustrated in Figure 1.

The influence of polymer structure and film morphology may also be seen by comparison of the charge-transport rates for **3–6**

(37) Nielson, R. M.; McManis, G. E.; Safford, L. K.; Weaver, M. J. *J. Phys. Chem.* **1989**, *93*, 2152.

(38) Daum, P.; Murray, R. W. *J. Phys. Chem.* **1981**, *85*, 389.

with those for **1** and **2**. $D_o^{1/2}C$ values for **1** and **2** are in the range $(1.4–7.5) \times 10^{-8}$ mol/(cm^2 s$^{1/2}$),[8] which is an order of magnitude less than the maximum observed for the series of polymers reported here.

Conclusions

In conclusion, the synthetic approach illustrated by eq 1 provides a route to phosphazene polymers with ferrocene substituents at various intervals which are attached to the polymer backbone by flexible carbon spacer groups. Reversible electrochemistry is observed for **3–6**. We have established that increasing the number of ferrocene substituents increases the charge-transfer efficiency for the phosphazene polymer in solution and as a film deposited on an electrode surface. This trend is consistent with an increasing contribution to the observed diffusion coefficient by electron hopping. Results reported here for **3–6** are more directly comparable to those for **2** than to those for **1**, the latter of which exhibits irreversible electrochemistry, apparently as a result of its transannular structure.[8] Apparently the flexible carbon spacer groups in **3–6**, relative to **2**, improve the charge-transport efficiency of the polymer.

Acknowledgment. We thank the Robert A. Welch Foundation, the U.S. Army Research Office, and the Duke University Research Council for generous financial support of this project. We also thank Dr. John Banewicz (SMU) for performing the elemental analyses, Dr. Maneesh Bahadur for molecular weight measurements, Dr. Fethi Bedioui (Ecole National Superieure de Chimie de Paris) for helpful discussions, and Dr. Louis A. Coury, Jr. (Duke), for helpful discussions and the use of the RDV equipment.